Search for $K_L \to 3\gamma$

June 10, 2007

1 Introduction

$K_L \to 3\gamma$ is a CP allowed decay, but gauge invariance and Bose statistics gives it a theoretically predicted branching ratio of 3×10^{-19}[1]. The only existing experimental limit on this branching ratio was done by the NA31 experiment at CERN SPS, who set a limit of 2.4×10^{-7}[2]. This report is about a search for the decay in one week of Run 2 data of the E391a experiment.

2 Reconstruction

To calculate the z-vertex of the kaon, I employ the formula used by [2]:

$$z_K = z_{CsI} - \frac{1}{m_K}\sqrt{\sum_{i,j,i<j} E_i E_j \left(\vec{r_i} - \vec{r_j}\right)^2}$$

Where $z_{CsI} = 614.8$ cm is the z position of the CsI detector, m_K is the kaon mass, E_i, E_j are the photon energies, and $\vec{r_i}, \vec{r_j}$ are the position vectors of the impact points of the photons.

3 Photon Vetoes

The cut values used for these vetoes were determined by either comparing their effects on signal events generated by Monte Carlo with background events ($K_L \to 2\pi_0$ 3-cluster events) or by observing their effects on the signal-to-noise ratio of $K_L \to 2\pi_0$ events. The photon and gamma quality vetoes are as follows:

Veto	Cut Value	Data Time Window	MC Time Window	Signal Acceptance
Front Barrel	0.8 MeV	(16.1, 48.2)	(-35.9, 15.7)	0.989
CC02	0.5 MeV	(-32.9, -14.3)	(-20.3, -1.7)	0.999
CC03	1.3 MeV	(-83.9, -51.0)	(-21.8, 14.4.)	0.984
CC04 Charge	2 MeV	(-25.0, 10.0)	(-14.0, 21.0)	0.982
CC04 Calorimeter	5 MeV	(-6.4, 5.0)	(-2.0, 9.4)	0.972
CC05 Charge	2 MeV	(-3.0, 7.8)	(3.8, 14.6)	0.997
CC05 Calorimeter	2 MeV	(3.2, 11.6)	(5.1, 13.5)	0.986
CC06	9 MeV	(-10.0, 25.0)	(-6.9, 28.1)	0.990
CC07	9 MeV	(-4.7, 27.7)	(-3.2, 29.2)	0.991
Charge Veto	1 MeV	(-15.3, 12.9)	(-12.1, 16.1)	0.903
Barrel Charge Veto	0.5 MeV	(18.1, 66.5)	(-26.0, 38.8)	0.710
Main Barrel	2 MeV	(-304, -150)	(4.0, 10.0)	0.750
BA Quartz E-Sum	1 MIPS	None	None	0.768
CsI Vetoes				
CsI In-time E-Sum	20 MeV	(-2, 8)	(-2, 8)	0.931
CsI Out-time E-Sum	10 MeV	(-2, 8)	(-2, 8)	0.899
Gamma Time Window	N. A.	(-2, 8)	(-2, 8)	0.960
Min. Gamma Energy	20 MeV	N. A.		0.826

Note:

1. For all analyses in this report, only events with decays within the fiducial region (300cm $< z_K <$ 500cm) were counted.

2. The main barrel and barrel charged veto cuts were done not only on the energy deposited in any single channel, but also on the sum of energies in pairs of upstream-downstream channels. This eliminated events where energy from one photon was deposited across a pair of upstream-downstream modules and where the individual deposits in each module were below the cut point but their sum was above the cut point.

3. All acceptances except for the BA were calculated by turning off all vetoes except the one in question and recording the proportion of signal events left as a result of the single veto applied. As the Monte Carlo still does not simulate BA events accurately, the acceptance of the BA veto was estimated as the acceptance of $K_L \to 2\pi_0$ signal events for the same veto. The latter was done by isolating signal events of $K_L \to 2\pi_0$ in one week of Run 2 4-cluster data and applying the BA veto to them.

4 Kinematic Vetoes

4.1 Gamma Radius Cut

Due to energy leakages near the edge and center of the CsI, we ignore events with photon impacts less than 19.5 cm or more than 93 cm from the center of the CsI. This cut has an acceptance of 0.786.

4.2 Transverse Momentum (p_T)

The expected background of three photons from $K_L \to 2\pi_0$ should reveal missing transverse momentum from the fourth undetected photon, whereas transverse momentum should be zero for signal events. This difference can be seen in the Monte Carlo simulations of signal and background events:

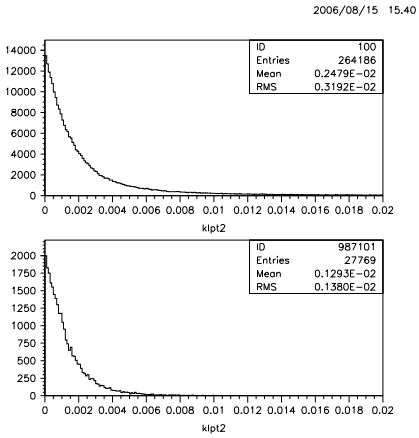

Figure 1: Comparison of the transverse momentum of background events (top) and signal events (bottom)

We cut all events with $p_T^2 > 0.001$ GeV^2. The acceptance for this cut is 0.538 for signal events and 0.474 for background events.

4.3 Reconstructed π_0 z-vertex cut

This cut was used by the NA31 group.

We reconstruct the z-vertex of a putative π_0 that decays into two of the detected photons, using the following formula:

$$z_{\pi_0} = z_{CsI} - \frac{1}{m_K}\sqrt{E_i E_j \left(\vec{r_i} - \vec{r_j}\right)^2}$$

where $\vec{r_i}, \vec{r_j}, E_i and E_j$ are the position vectors and the energies of the photons in the pair chosen.

For a 3-photon event, there are three possible combinations. These are all calculated, and ranked according to the magnitude of z_{π_0}. Monte Carlo

simulations of our expected background, 3-photon events from the $K_L \to 2\pi_0$ decay, show a correlation between z_K and the largest magnitude of z_{π_0} (Fig. 2). No such correlation is found for Monte Carlo simulations of signal events (Fig. 3). Events that satify the following conditions are cut:

$$\frac{23}{19} z_K - 168 < z_{\pi_0,1} < \frac{15}{14} z_K - 5$$

where $z_{\pi_0,1}$ is the maximum reconstructed z_{π_0} and z_K is the reconstructed K_L z-vertex.

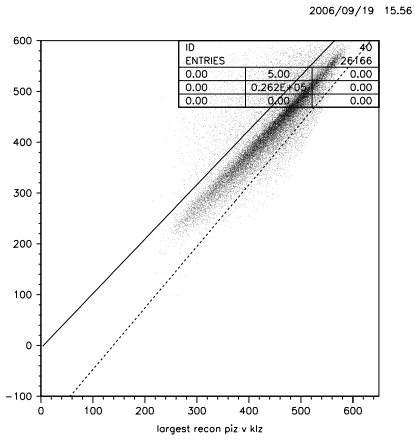

Figure 2: $z_{\pi_0,1}$ plotted against z_K for MC background (3-cluster $K_L \to 2\pi_0$) events, after all photon vetoes, CsI vetoes, gamma quality vetoes, and the p_T veto.

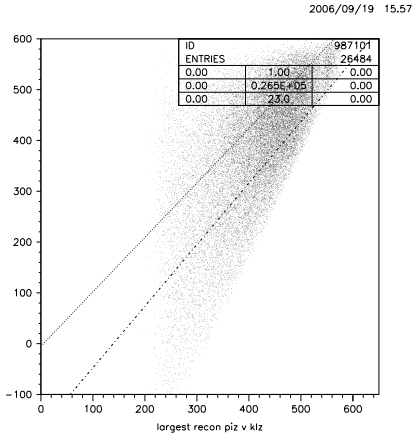

Figure 3: $z_{\pi_0,2}$ plotted against z_K for MC signal events, after all photon vetoes, CsI vetoes, gamma quality vetoes, and the p_T veto.

The above cut eliminated 86% of $2\pi_0$ 3-cluster events and 45% of 3γ signal events.

A second cut based on the same principle can be made. For the remaining events left after the cut on the correlation between z_K and the largest magnitude of z_{π_0}, we find a correlation between the second largest magnitude of z_{π_0} andz_K in the background, but not in the signal (Figs. 4, 5). Events that satify the following conditions are cut:

$$\frac{6}{5}z_K - 165 < z_{\pi_0,2} < \frac{40}{39}z_K - 5$$

where $z_{\pi_0,2}$ is the second largest reconstructed z_{π_0}.

This cut eliminated 61% of the remaining $2\pi_0$ 3-cluster events and 10% of the remaining 3γ signal events.

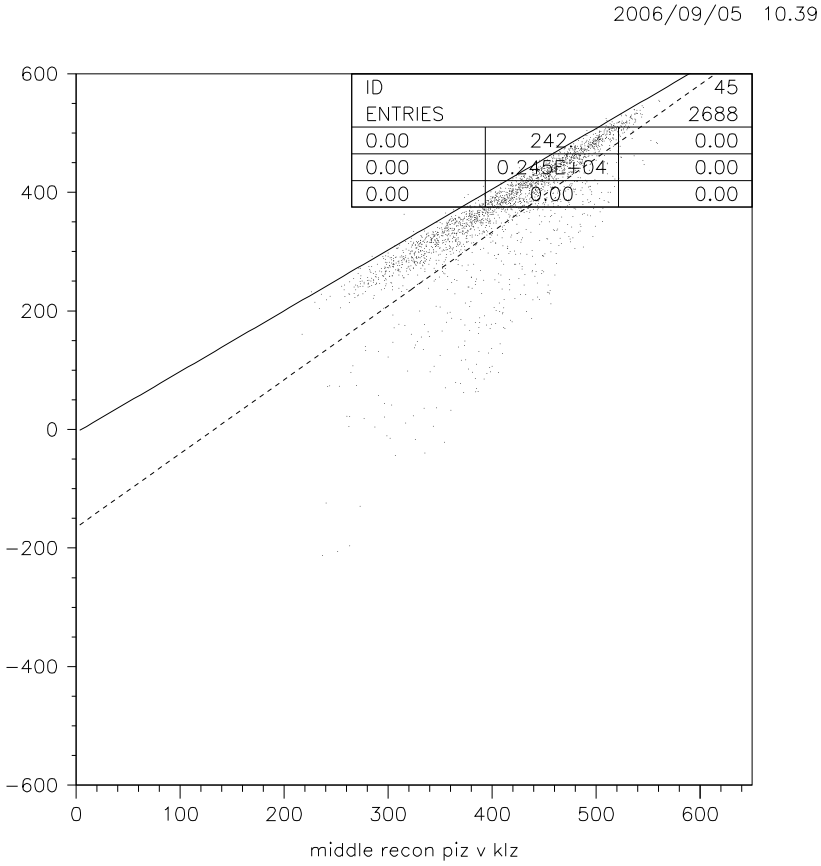

Figure 4: $z_{\pi_0,2}$ plotted against z_K for MC background (3-cluster $K_L \to 2\pi_0$) events, after all photon vetoes and the first cut on $z_{\pi_0,1}$.

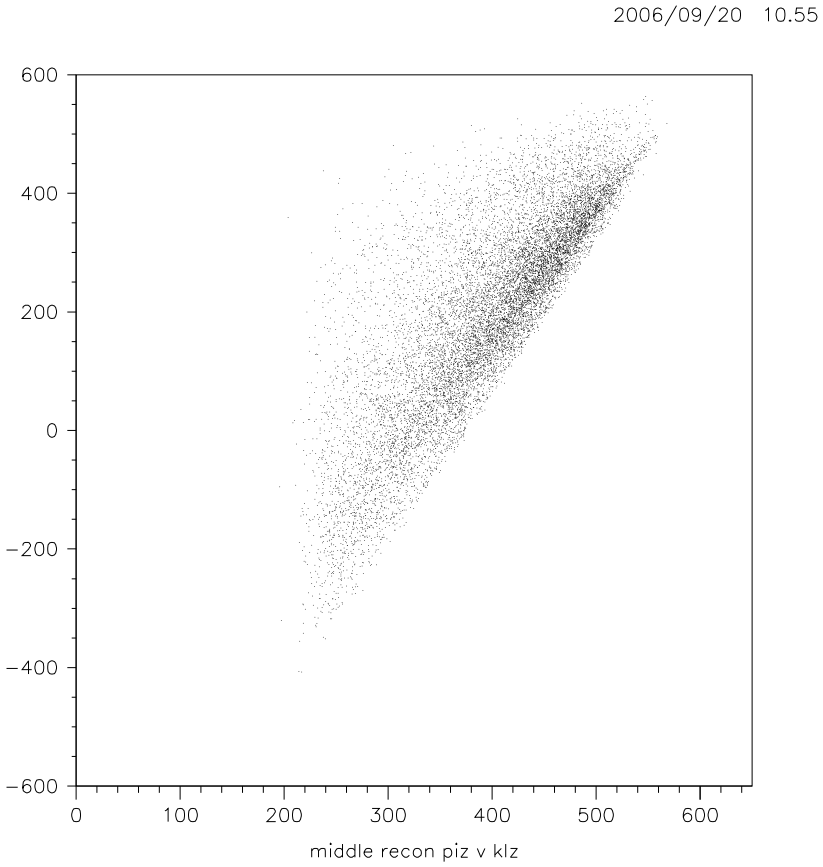

Figure 5: $z_{\pi_0,2}$ plotted against z_K for MC signal events, after all photon vetoes and the first cut on $z_{\pi_0,1}$.

4.4 Neural Net Fusion Cut

This was set to cut all events with a neural net fusion value of less than 0.7. The acceptance of this cut is 63%.

4.5 Kinematic Fusion Cut (not used)

The following cut was used by NA31 to remove fusion events. One of the photon energies, E_j, was assumed to be the sum of two overlapping photons from a $K_L \to 2\pi_0$ event, with $k_1 E_j$ coming from one pion and $(1-k_2)E_j$ coming from the other. Fusion events occur when $k_1 = k_2$. We use the known π_0 mass and the equations

$$z_{\pi_0} = \frac{1}{z_{CsI} - z_K} \times \sqrt{E_i k_1 E_j \left(\vec{r_i} - \vec{r_j}\right)^2}$$

and

$$z_{\pi_0} = \frac{1}{z_{CsI} - z_K} \sqrt{E_i \left(1 - k_2\right) E_j \left(\vec{r_i} - \vec{r_j}\right)^2}$$

to calculate three possible values (for each possible E_j) of k_1 and k_2. The minimum of the three values of $|k_1 - k_2|$ is plotted for both signal and background:

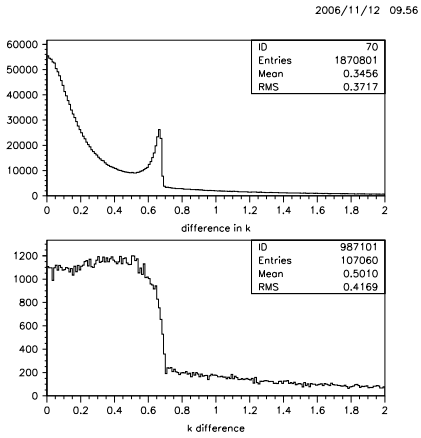

Figure 6: **Top**: Minimum $|k_1 - k_2|$ for background ($K_L \to 2\pi_0$ 3-cluster events). **Bottom**: Minimum $|k_1 - k_2|$ for $K_L \to 3\gamma$ events.

As expected, the background events show a much higher incidence of low values of $|k_1 - k_2|$ than the signal events. This would therefore be a potentially powerful cut. However, it overlaps almost completely with the other photon and kinematic cuts: Fig. 7 shows the minimum $|k_1 - k_2|$ after all other cuts and the low minimum $|k_1 - k_2|$ events in the noise have been almost completely eliminated by the other cuts, such that applying it would not have further improved the signal to noise ratio. Therefore this cut was not used in my analysis.

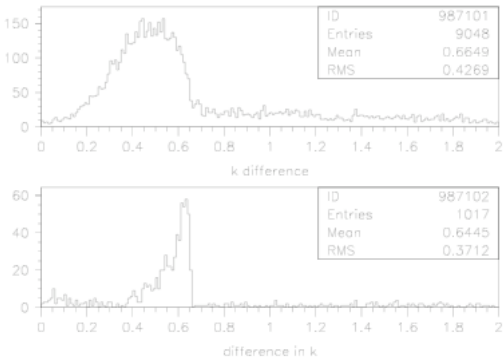

Figure 7: $|k_1 - k_2|$ after all other photon and kinematic vetoes. **Top**: Minimum $|k_1 - k_2|$ for signal. **Bottom**: Minimum $|k_1 - k_2|$ for background.

4.6 Summary

The relative impact of each veto is summarised in the following graph:

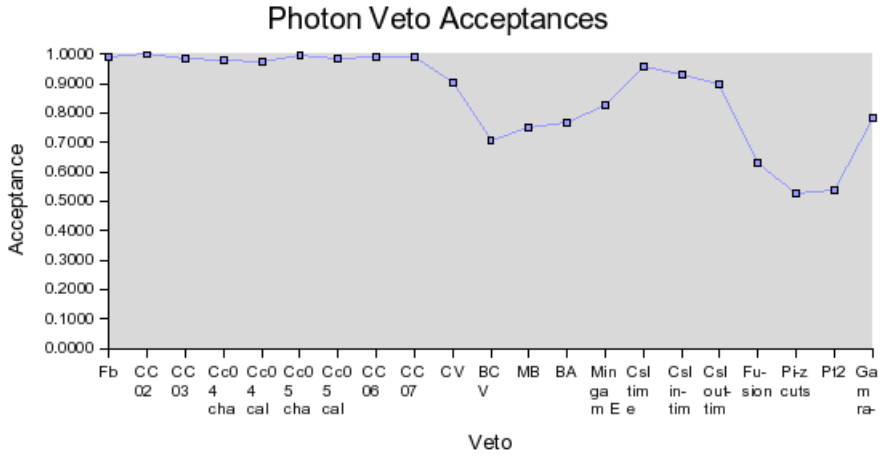

5 Results

5.1 Flux

Flux was calculated using the same photon vetoes on $K_L \to 2\pi_0$ signal events. Using these photon vetoes and the usual kinematic cuts (p_T and mass peak), 16295 events were left out of a Monte Carlo sample of 12×10^6 decays, giving an acceptance of 0.00136. Applying the same cuts to one week of Run 2 data, we get 570 signal events. Since the branching ratio of $K_L \to 2\pi_0$ is 0.000865, the one week kaon flux is $\frac{570}{0.000865 \times 0.00136} = 4.85 \times 10^8$.

5.2 Signal Acceptance and Sensitivity

This was calculated using a Monte Carlo sample of pure $K_L \to 3\gamma$ decays, with accidental overlay.

Size of Monte Carlo sample generated: 4.2×10^7 at C6
Decay probability: 2.4%
No. of events left after all vetoes except BA: 8157
BA Acceptance: 0.768
Acceptance: $\frac{8157 \times 0.768}{0.024 \times 4.2 \times 10^7} = 0.00621$
Single event sensitivity, $SES = \frac{1}{0.00621 \times 4.85 \times 10^8} = 3.32 \times 10^{-7}$

5.3 Data

From 3-photon events in one week (runs 3950-4050) of Run 2 data, we get 3 remaining events in the p_T^2 vs z signal region:

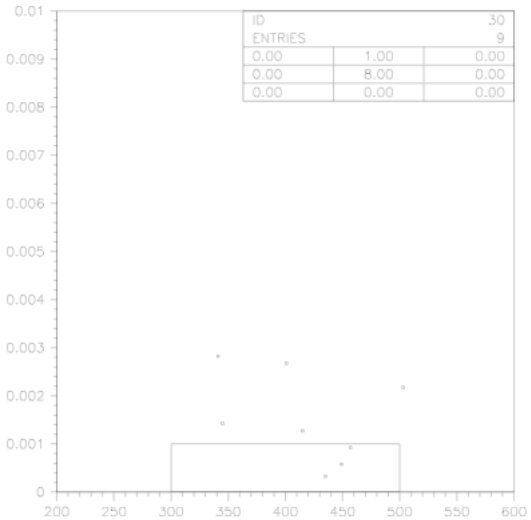

Figure 8: p_T^2 vs z plot for 1 week data, signal region boxed

5.4 Background Estimate

This was estimated by assuming that 3-cluster events from $K_L \to 2\pi_0$ decays, in which the fourth photon either fused with one of the three that hit the CsI or hit some other detector, are responsible for most of the background. Thus a Monte Carlo sample of $K_L \to 2\pi_0$ events with accidental overlay was generated, and the 3-cluster events amongst those were chosen for this analysis.

Size of MC sample generated: 1×10^8 at C6

Decay probability: 2.4 %

No. of events left after all vetoes except BA: 57

BA Acceptance: 0.768

Acceptance: $\frac{57 \times 0.768}{0.024 \times 10^8} = 1.82 \times 10^{-5}$

Expected background $= 1.82 \times 10^{-5} \times 0.000865 \times 4.85 \times 10^8 = 7.65$ events.

This is more than twice the number of events found in the data. In the next section I suggest possible sources of this discrepancy.

6 Outstanding Problems

6.1 The CsI Timing Issue

The timing function in the data has a fairly broad spread, whilst that in the Monte Carlo is practically a delta function (Figs. 9, 10).

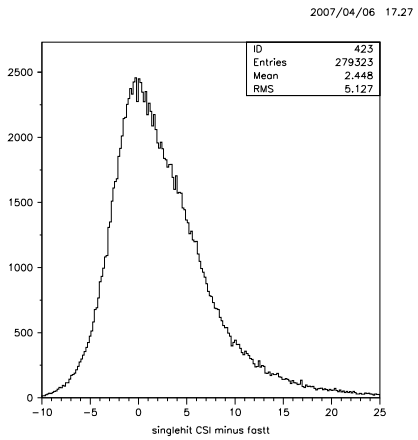

Figure 9: Time after fastest gamma, $K_L \to 2\pi_0$ signal in Run 2 data

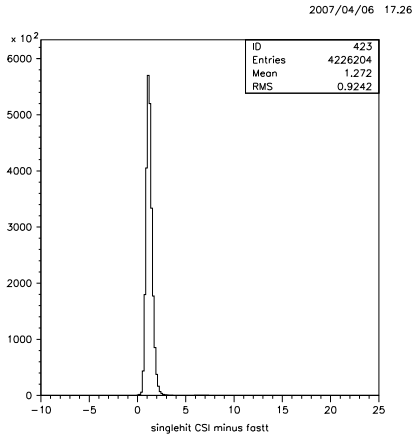

Figure 10: Time after fastest gamma, $K_L \to 2\pi_0$ signal in Run 2 MC

To check the effects of this discrepancy of the timing function, we calculated, for from $K_L \to 2\pi_0$ signal events, the proportion of total energy deposits in the CsI that was in the gamma clusters. The proportion of such "extra" energy in the CsI in the time window of (-2, 8) does not have the same profile in the Monte Carlo and the data (Figs. 11, 12).

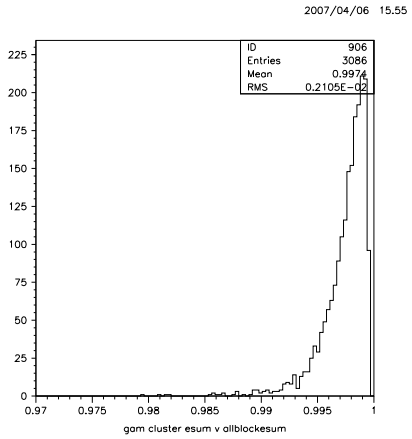

Figure 11: $2\pi_0$ data signal inside time window (-2, 8): Number of events versus proportion of total energy in CsI due to gamma clusters

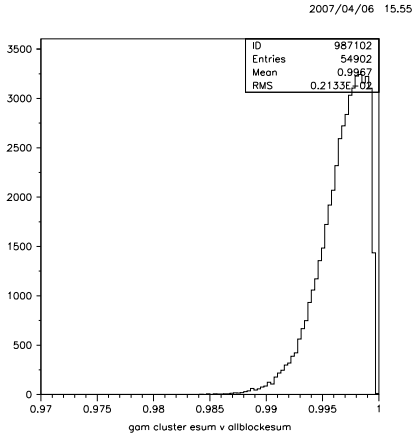

Figure 12: $2\pi_0$ MC signal inside time window (-2, 8): Number of events versus proportion of total energy in CsI due to gamma clusters

Clearly, the (-2, 8) time window removes skews the event distribution in the data towards events with less energy deposits outside the gamma clusters: the MC has relatively more events with "extra" energy.

If we expand the time window to (-5, 15), the discrepancy between data and Monte Carlo is reduced:

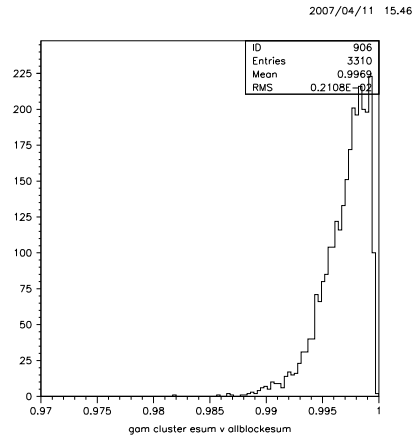

Figure 13: $2\pi_0$ data signal inside time window (-5, 15): Number of events versus proportion of total energy in CsI due to gamma clusters

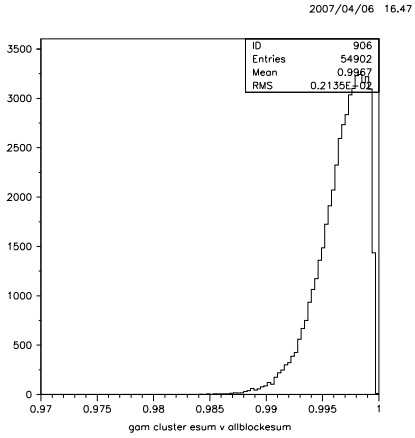

Figure 14: $2\pi_0$ MC signal inside time window (-5, 15): Number of events versus proportion of total energy in CsI due to gamma clusters

6.2 Main Barrel Energy Calibration

The main barrel is another possible source of discrepancy, and is particularly important due to its large effect on acceptance. We looked at events in the data that had 5 in-time photons hitting the CsI and had no energy deposits anywhere but the main barrel (in other words, we applied all photon and fusion vetoes except for that of the main barrel). These should be almost entirely due to the decay $K_L \to 3\pi_0 \to 6\gamma$ with one photon in the main barrel. Thus, we should get the same energy spectrum in the main barrel if we compare it to Monte Carlo samples of $K_L \to 3\pi_0 \to 6\gamma$ that have 5 photons hitting the CsI and negligible energy deposits in any other detector except the main barrel. However, the MC and data energy spectra for such events differ significantly (Figs. 15, 16):

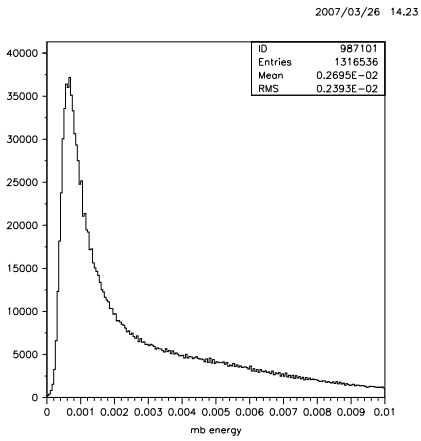

Figure 15: In-time MB energies of 5-cluster events in Run 2 data with all photon vetoes except MB applied.

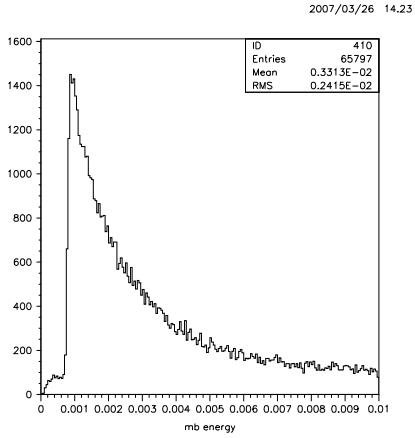

Figure 16: In-time MB energies of 5-cluster events in Run 2 MC with all photon vetoes except MB applied.

The discrepancy between MC and data also shows up in the distribution of maximum energies in the MB (Figs. 17, 18). Given this discrepancy, we cannot be sure that the MB acceptance as calculated from MC samples accurately reflects the MB acceptance in the real data.

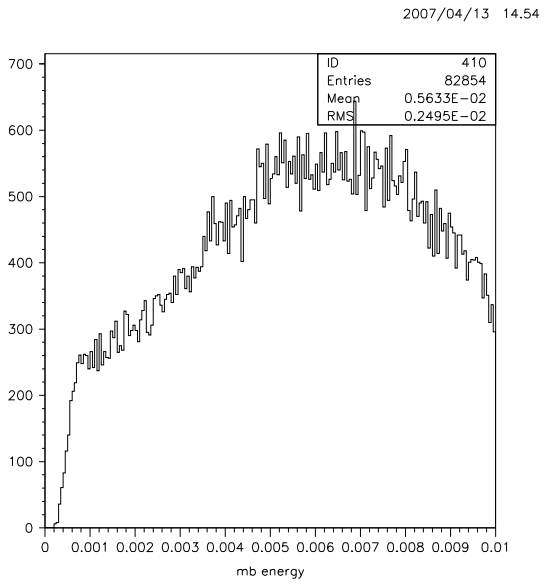

Figure 17: In-time **maximum** MB energies of 5-cluster events in Run 2 data with all photon vetoes except MB applied.

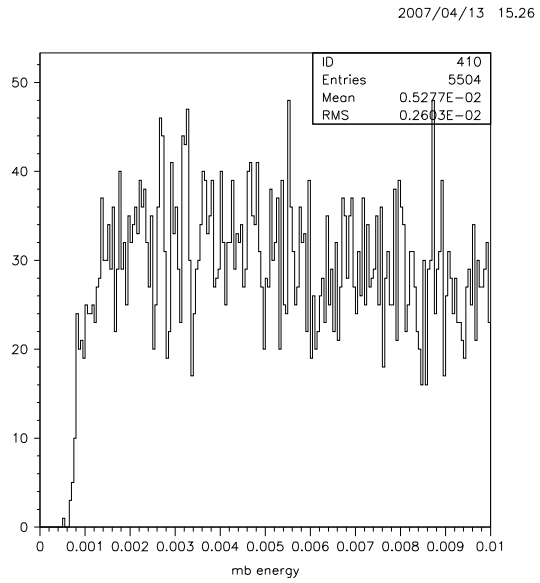

Figure 18: In-time **maximum** MB energies of 5-cluster events in Run 2 MC of $K_L \to 3\pi_0$ with all photon vetoes except MB applied.

References

[1] P. Heiliger, B. McKellar and L. M. Sehgal, Phys. Lett. B 327 (1994) 145.

[2] G. D. Barr et al., Phys. Lett. B 358 (1995) 399.